ELSEVIER

PII: S0032-3861(96)00919-6

Polymer Vol. 38 No. 14, pp. 3609–3616, 1997

0032-3861/97/$17.00 + 0.00

Polymerization of polyurethane and vinyl ester resin interpenetrating polymer networks during reaction injection moulding process*

Lian Hua Fan, Chun Pu Hu†, Zhao Qi Pan, Zhi Ping Zhang and Sheng Kang Ying

Institute of Material Science and Engineering, East China University of Science and Technology, 130 Meilong Road, Shanghai 200237, P.R. China

(Revised 23 September 1996)

The reaction kinetics of polyurethane and vinyl ester resin interpenetrating polymer network (PU/VER SIN) during reaction injection moulding (RIM) polymerization has been on-line monitored by using a Fourier transform infrared (*FT*i.r.) spectrometer linked up with a portable mini-RIM machine. For using VER, in which the pendent hydroxyl groups were capped with acetyl groups to minimize the possibility of chemical binding between the two networks, the two pairs of reactants interfere with each other during the course of synthesis. The unusual polymerization kinetics behaviour observed could be correlated well with the change of morphology of the system. For using VER containing pendent hydroxyl groups, the occurrence of chemical binding between the two networks could greatly affect the reaction kinetics and morphology of the system. ©1997 Elsevier Science Ltd.

(Keywords: reaction injection moulding; polyurethane; vinyl ester resin)

INTRODUCTION

Reaction injection moulding (RIM) process is the high speed production of polymer parts directly from low viscosity reactants injected into a mould. The major development of RIM material has been in the polyurethane (PU) area since it was first commercialized in 1975. To improve the performance of RIM products, Pernice and co-workers first reported simultaneous interpenetrating networks (SINs) composed of PU and industrial unsaturated polyester resin or epoxy resin for applying in RIM technology[1]. Since then there has been increasing interest in using SINs as RIM materials. Most of the studies were related to SINs composed of PU and unsaturated polyester resin[2–7]. However, the interaction between these two constituent components has not been examined in detail, as the hydroxyl and carboxyl end groups of polyester chains are easy to react with isocyanates.

Our group has explored another kind of SINs composed of PU and vinyl ester resin (VER), which could be used in RIM process[8,9]. As VER is also possessed of pendent hydroxyl groups on its backbones, the inter-component chemical binding effect between the two networks has been studied and it has been found that the kinetics of PU/VER SIN formation is greatly affected by the hydroxyl groups existing in VER[10,11]. Furthermore, the mechanical properties for these SINs, in which the hydroxyl groups of VER are capped or not capped with acetyl groups, are found to be completely different[12]. In the present paper, the polymerization of PU/VER SINs during RIM process is reported. The unusual kinetics behaviour for such a fast polymerization could be correlated well with the change of morphologies during the formation of these SINs.

EXPERIMENTAL

Material

Trifunctional poly(oxypropylene) polyol [GH-330E, hydroxyl number (HN): 57 mg KOH g^{-1}] was supplied by GaoQiao No. 3 Chemical Plant. The uretonimine modified liquid MDI (L-MDI) was provided by Institute of Liming Chemical Technology. All other chemicals used in this study were standard laboratory reagents obtained from various manufacturers.

The polyol was dried at 100°C under vacuum for 12 h, then treated with 4 Å molecular sieves for over one week before use. 1,4-Butanediol (1,4-BDO) was distilled under vacuum in the presence of sodium wire. Styrene was washed, dried and distilled under vacuum, and inhibited with 1,4-hydroquinone (0.01 phr). Benzoyl peroxide (BPO) was first dissolved in chloroform. The solution was dried with anhydrous sodium sulfate and filtered. Then BPO was recrystallized from methanol, and dried under vacuum at room temperature.

PU was formed from polyol GH-330E, isocyanate L-MDI and chain extender 1,4-BDO with hard segment content of 45% (based on total mass of L-MDI and 1,4-BDO). The catalyst for PU, dibutyltin dilaurate

* Project supported by National Natural Science Foundation of China
† To whom correspondence should be addressed

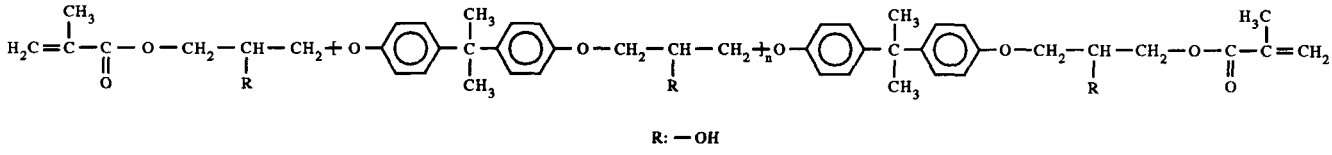

R: —OH

Figure 1 Structural formula of vinyl ester oligomer (VEO)

Table 1 Processing conditions and chemical systems for RIM PU/VER SINs

Metering ratio	Chemical system	Component A		Component B	
		Material	Temperature	Material	Temperature
0.53	PU	L-MDI	30°C	GH-330E, BDO, DBTDL	60°C
1/0.53	PU/VERA SIN	L-MDI, VERA, BPO	30°C	GH-330E, BDO, DBTDL, DMA	60°C
1.00	VERA	VERA, BPO	30°C	VERA, DMA	30°C
0.35	PU/VERH SIN	L-MDI, DMA	60°C	GH-33OE, BDO, DBTDL, VERH, BPO	30°C

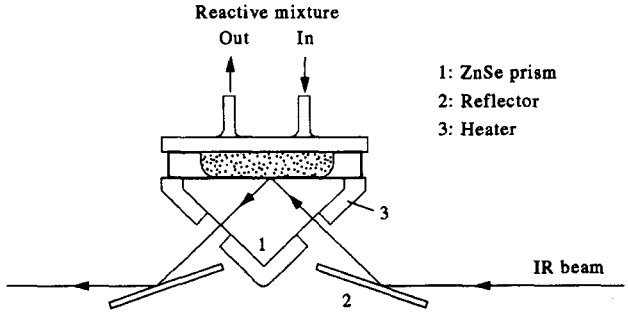

Figure 2 Schematic drawing of prism liquid cell used in on line *FT*i.r. measurements

(DBTDL), was used as received at 0.75 phr (by weight of polyol). Vinyl ester resins were first prepared by the adduction reaction of 1 mole bisphenol A type epoxy resin E-51 (0.513 epoxide equivalent/100 g resin) supplied by Shanghai Synthetic Resin Plant and 2 mol α-methacrylic acid to get vinyl ester oligomer (VEO). *Figure 1* shows the structural formula of VEO. Styrene (St) as comonomer was then introduced into this VEO (VEO/St = 64/36, weight ratio). The resulting VER was designated as VERH, as such a VEO was possessed of pendent hydroxyl groups. To obtain the so-called VERA, in which the pendent hydroxyl groups were capped with acetyl groups, a suitable amount of acetyl chloride was added in drops to VEO. The system was exposed to vacuum to eliminate hydrochloride and finally combined with styrene. All procedures for preparation and characterization of VERH and VERA have been described elsewhere[10,11]. In order to start the free radical copolymerization fast enough for matching the RIM process, we employ a redox initiator system instead of 2,2-azo-bisisobutyronitrile (AIBN) as used previously[10,11]. The initiator BPO and promotor N,N-dimethyl aniline (DMA) were set at 4 phr and 1 phr of VER, respectively.

Instrumentation

A mini-RIM machine was designed by our group to interface with analytical instruments. The stoichiometric ratio of reactants is controlled by the diameters of the two reactant cylinders and a fixed cross arm; and thus the ratio is not continuously variable, but is changed in steps by the diameters (diameter ratio squared) of the reactant cylinders. The cylinders are driven pneumatically at a controllable rate to achieve good impingement mixing. Temperature control of reactants is maintained by the heating tapes wrapped around these cylinders with a type K (nickel–chromium vs nickel–aluminium silicon) thermocouple immersed in the reactants at an accuracy of ±1°C. For preparation of PU, VER networks and PU/VER SINs, the raw materials were divided into two parts (Component A and Component B) and put into the two cylinders, respectively, as shown in *Table 1*.

A Nicolet 5SXC *FT*i.r. spectrometer was employed for *in situ* kinetics measurements. A prism liquid cell was installed in the sample compartment of the *FT*i.r. spectrometer, as shown in *Figure 2*. A ZnSe prism with 45°–90°–45° angles was used for single bounce internal reflection measurement at desired reaction temperature, which was controlled by a type K thermocouple inserted in the heating plate of the prism liquid cell at an accuracy of ±1°C. The liquid cell was aligned for i.r. beam reflection by adjusting the two reflectors. The outlet of the RIM machine mixhead was connected to the inlet of the liquid cell through ϕ6 mm nylon tube. The loading time of impingement mixed reactants into the prism liquid cell was typically only about 0.3 s.

I.r. spectra with 4 cm^{-1} resolution can be collected at intervals of around 0.59 s with a reasonable signal to noise ratio, which permits the determination of the concentrations of the absorbing species in the reaction medium, upon the use of Beer–Lambert law,

$$A = \varepsilon c l$$

where A is the absorbance, ε is the molar extinction efficient, c is the concentration of the absorbing species, and l is the thickness of the test sample. In the reflection mode, the i.r. absorption is limited to the sample near the prism surface; and specifically for our measurement

Table 2 Polymerization parameters of PU formation

Temperature (°C)	RIM PU		PU in RIM PU/VERA(53/47) SIN	
	Initial reaction rate ($mol\,l^{-1}\,s^{-1}$)	−NCO conversion (at 30 s)	Initial reaction rate ($mol\,l^{-1}\,s^{-1}$)	−NCO conversion (at 5 min)
60	0.245	0.65	0.053	0.73
70	0.350	0.68	0.067	0.77
80	0.490	0.72	0.082	0.81
90	0.711	0.76	0.099	0.87
100	1.091	0.79	0.120	0.92

configuration the approximate depth of penetration of the i.r. absorption goes 0.7 μm[13]. Therefore, the measured data represent the reaction profile of the resin near the mould surface. To compensate for the change of optical contact between the sample and the prism surface during polymerization, a ratio is taken between the absorbance of the group of interest and that of an internal standard, i.e. a group whose concentration does not change during reaction course. In this study, the C−H peak at 2942 cm^{-1}, and the phenyl peak of styrene at 700 cm^{-1} are chosen as the internal standard for polyurethane[3], and styrene as well as all SINs[14], respectively. The absorbance area determined by the tangent baseline method[13,15] is used to calculate the reaction conversion from the change of the normalized absorbance,

$$\alpha = 1 - A_t/A_0$$

where A_0 and A_t are normalized absorbance of the monomer functional group before the reaction and after a reaction time t.

Differential scanning calorimetry (d.s.c.) was measured with a DuPont Instrument 1090 thermal analyzer at a heating rate of 10°C min^{-1}.

RESULTS AND DISCUSSION

Polymerization of RIM PU

The isocyanate group conversion (α) of RIM PU polymerization at different temperatures can be obtained from absorbance change at 2274 cm^{-1} [3,16,17] and is shown as a function of reaction time in *Figure 3*. The value of $1/(1-\alpha)$ obtained from *Figure 3* against time is shown in *Figure 4*, where the straight lines with their intercepts of 1.0 reveal that the disappearing rate of isocyanate groups in RIM PU polymerization is simply expressed as:

$$-\mathrm{d[NCO]}/\mathrm{d}t = k[\mathrm{NCO}][\mathrm{OH}]$$

or

$$-\mathrm{d[NCO]}/\mathrm{d}t = k[\mathrm{NCO}]^2$$

because of initial reactants in stoichiometric ratio, i.e. [NCO] = [OH]. The overall reaction kinetics can be written in terms of conversion, $\alpha = ([\mathrm{NOC}]_0 - [\mathrm{NCO}]_t)/[\mathrm{NCO}]_0$,

$$\mathrm{d}\alpha/\mathrm{d}t = k[\mathrm{NCO}]_0(1-\alpha)^2$$

thus

$$1/(1-\alpha) = k[\mathrm{NCO}]_0 t + 1$$

Figure 4 indicates that the reaction between −NCO and −OH groups follows second order reaction kinetics at early period. However, the reaction deviates from second order reaction kinetics at around 40–50% isocyanate conversion as a result of phase separation of urethane hard segment sequence lengths. The reaction kinetics goes from second order to diffusion control. With the increase of reaction temperature, the early step polymerization rate of PU as well as the −NCO conversion at a given reaction time increase, as listed in *Table 2*.

The inter-urethane hydrogen bonding can be characterized in the carbonyl region between 1800 cm^{-1} and

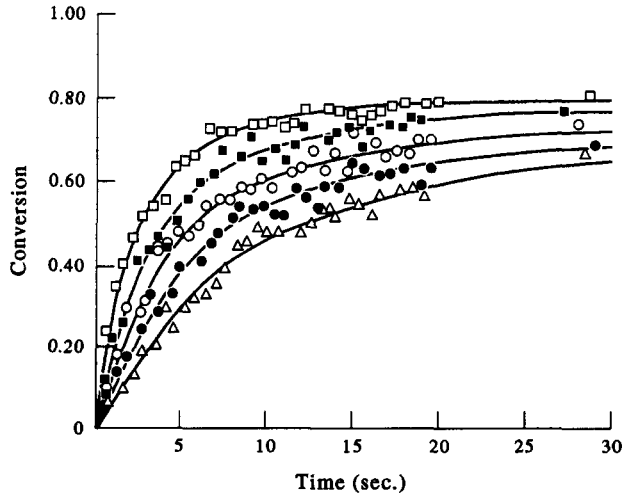

Figure 3 Conversion of −NCO vs time for RIM PU at different temperatures: □, 100°C; ■, 90°C; ○, 80°C; ●, 70°C; △, 60°C

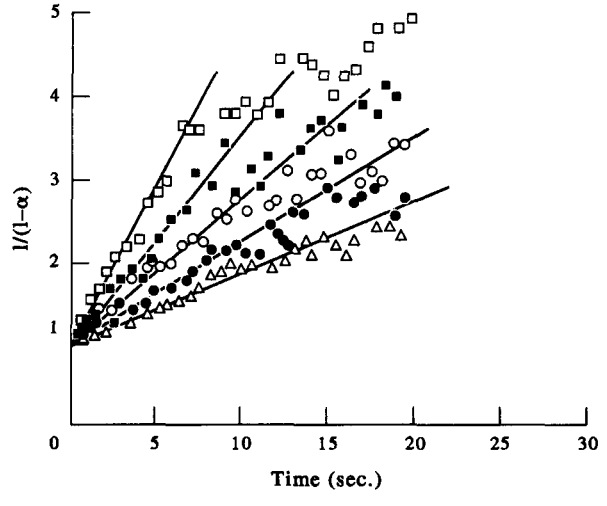

Figure 4 $1/(1-\alpha)$ vs time plot for RIM PU at different temperatures: □, 100°C; ■, 90°C; ○, 80°C; ●, 70°C; △, 60°C

Table 3 Copolymerization parameters of VERA formation

Temperature (°C)	RIM VERA			VERA in RIM PU/VERA(53/47) SIN		
	Induction period (min)	$d\alpha/dt$ (s^{-1})	Styrene conversion (at 5 min)	Induction period (min)	$d\alpha/dt$ (s^{-1})	Styrene conversion (at 5 min)
60	0.63	0.00618	0.78	1.51	0.00454	0.53
80	0.48	0.00764	0.68	0.95	0.00505	0.62
100	0.28	0.01180	0.62	0.33	0.00984	0.65

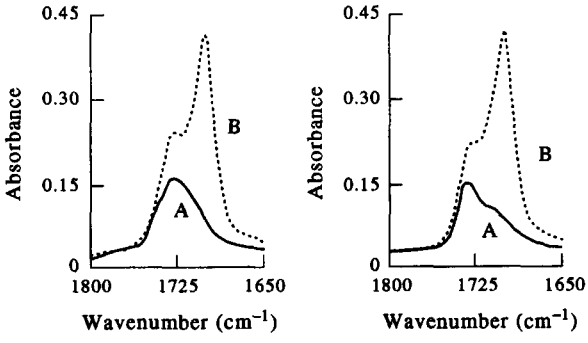

Figure 5 *FT*i.r. spectra in carbonyl region for RIM PU. Left: RIM PU at 60°C; right: RIM PU at 80°C. A, initial absorption; B, absorption at reaction time of 30 s

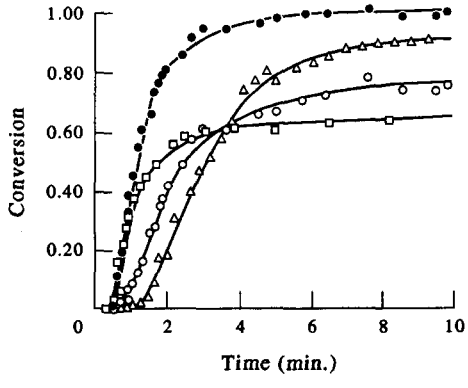

Figure 6 Conversion of copolymerization vs time in RIM VERA at different temperatures. Styrene comonomer: □, 100°C; ○, 80°C; △, 60°C. Acetyl group capped VEO: ●, 80°C

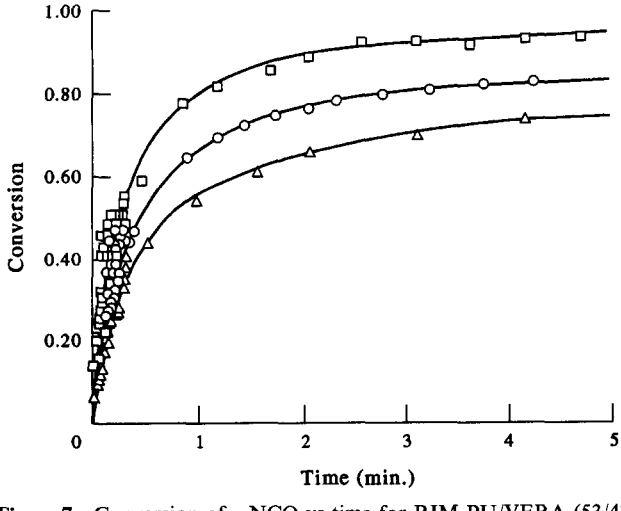

Figure 7 Conversion of –NCO vs time for RIM PU/VERA (53/47) SIN at different temperatures: □, 100°C; ○, 80°C; △, 60°C

1650 cm^{-1} during RIM PU polymerization by using *FT*i.r. *Figure 5* shows that the carbonyl absorption splits into two peaks during the polymerization of RIM PU, and the hydrogen bonded carbonyl absorption at 1705 cm^{-1} enhances with the increase of reaction time. Macosko and co-workers have indicated that phase separation between the soft and hard segments of PU should occur for enhancement of hydrogen bonding between the urethane linkages[16,18]. Bras *et al.*[19] also studied the phase separation of PU polymerization through simultaneous *FT*i.r. and SAXS measurements, however, found that the phase separation of the urethane hard segments took place before the onset of hydrogen-bonded urethane carbonyl formation. Nevertheless, during the phase separation of PU the hydrogen-bonded urethane carbonyl formation is in no doubt. Thus, the heterogeneous structure introduced into the reaction medium due to phase separation is the main reason to explain the change of polymerization mechanism during RIM process. In this case, the step polymerization between isocyanate and hydroxyl groups should be controlled by diffusion effect. As the polymerization temperature is raised, the rate of reaction increases and thus the time to reach α_{crit} (conversion of isocyanate group at the onset of phase separation) decreases. It is clear that the phase separation process occurs earlier at high temperature than at low temperature, so as to exhibit the onset of unusual kinetics behaviour of RIM PU much earlier at high temperatures.

Polymerization of RIM VERA

Figure 6 shows the conversions of the acetyl groups capped VEO (AGC-VEO) and styrene comonomer in RIM VERA copolymerization at different temperatures. The styrene conversion can be determined from the peak area change at 910 cm^{-1} [3,20]. Although the consumption of the double bonds on AGC-VEO cannot be followed directly from the peak at 1636 cm^{-1} [17,21], a subtraction method[3,20] was applied here to calculate the conversion of AGC-VEO.

It can be seen that the reactivity of the double bonds on AGC-VEO is higher than that of styrene monomer. However, the introduction of PU components to form RIM PU/VER SINs results in severe band overlapping in these wavenumber regions. Thus, the VEO double bonds have not been studied further for RIM SIN systems.

Similar to the mechanically mixed system studied previously[10], the kinetics curves of styrene display an almost linear correlation between conversion and time during the initial reaction stage, i.e. 10–30% conversion range, and the copolymerization rate of styrene ($d\alpha/dt$) can be estimated during this period, as listed in *Table 3*. It reveals an almost constant reaction rate during this

specific conversion range, that is to say, the copolymerization rates exhibit almost no dependence on the concentration of styrene comonomer. Thus, the unusual kinetics behaviour could be attributed to the strong diffusion restriction (translational and segmental diffusion) existing in this viscous network system[10,11,22].

Table 3 also shows that with increasing reaction temperature, the induction period decreases, and the value of $(d\alpha/dt)$ increases, but the copolymerization rate at later reaction stage as well as the final conversion level decreases (see *Figure 6*). This can be attributed to the much faster decomposition of BPO/DMA redox system at these rather high temperatures studied. O'Driscol *et al.*[23] have measured the decomposition rate constant of this redox system for styrene homopolymerization, i.e. $k_{d_{-2}} = 2.29 \times 10^{-3}\,l\,mol^{-1}\,s$ at 30°C and $k_d = 1.25 \times 10^{-2}\,l\,mol^{-1}\,s^{-1}$ at 60°C. As k_d increases appreciably with increasing temperature, much larger values of k_d could be expected at 80°C and 100°C in the present study (3.30×10^{-2} and $7.86 \times 10^{-2}\,l\,mol^{-1}\,s^{-1}$ at 80°C and 100°C, could be estimated respectively, assuming Arrhenius expression for k_d and temperature). Thus, the rate of initiation and the rate of polymerization of both monomers increase with increasing temperature, leading to the decreased induction period and increased $d\alpha/dt$ value during the initial reaction stage. Furthermore, such an initiator system will be depleted more quickly at higher temperature, which results in less initiator level available for initiating the free radical copolymerization at the later reaction stage. This, combined with the gelation-induced diffusion restriction of styrene polymerization upon the approaching of chemical network formation and possible vitrification effect, gives rise to the lowering of copolymerization rate at the later reaction stage as well as the reduced final conversion of styrene monomer.

Polymerization of RIM PU/VERA SINs

The reaction kinetics of PU and VERA in RIM PU/VERA (53/47, weight ratio) SIN at different temperatures are presented in *Figures 7* and *8*, respectively. The formation of PU networks is earlier than that of VERA network, and reaches fairly high conversion at about 1 min; while the conversion of styrene comonomer starts to level off at about 3 min. As the pendent hydroxyl groups in VERA are capped with acetyl groups, the RIM SINs composed of PU and VERA can be considered as more ideal ones with only minimum possibility of forming chemical bonds between the two networks. The analysis on the early data of PU polymerization in this RIM PU/VERA (53/47) SIN system still gives overall second order reaction kinetics, as shown in *Figure 9*. Nevertheless, *Table 2* shows that although the early step polymerization rate of PU increases with increasing temperature, it appears to be depressed in RIM SIN formation, compared with that in its pure system at the same temperatures. Because of the existence of the induction period of free radical copolymerization of VERA, the early stage of PU network formation reaction can be considered to take place in the diluents (VERA). Thus, decreasing the concentrations of PU reactants is the main reason for the depressed PU formation.

The occurrence of hydrogen bonding in this RIM PU/VERA (53/47) SIN system is also observed from *FT*i.r. spectra, as shown in *Figure 10*. With the consumption of isocyanate groups, the PU network forms quickly, and

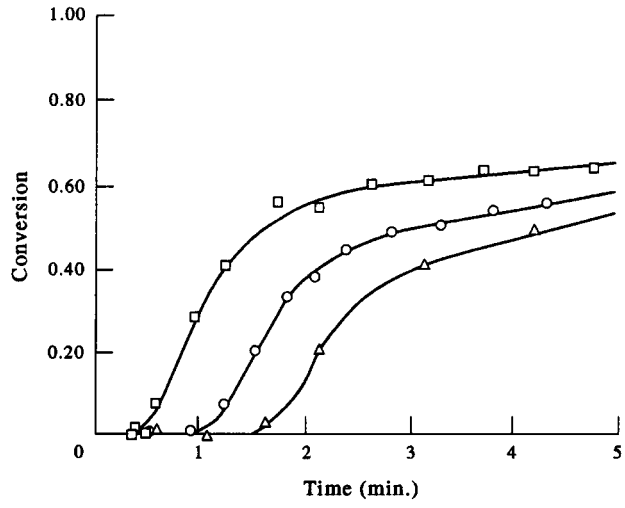

Figure 8 Conversion of styrene vs time for RIM PU/VERA (53/47) SIN at different temperatures: □, 100°C; ○, 80°C; △, 60°C

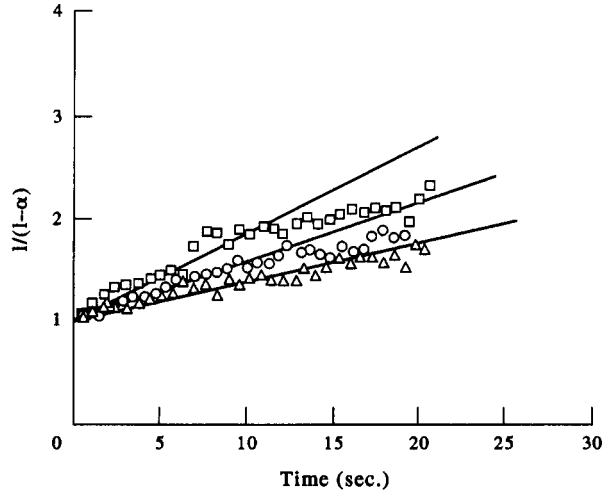

Figure 9 $1/(1-\alpha)$ vs time plot for PU in RIM PU/VERA (53/47) SIN at different temperatures: □, 100°C; ○, 80°C; △, 60°C

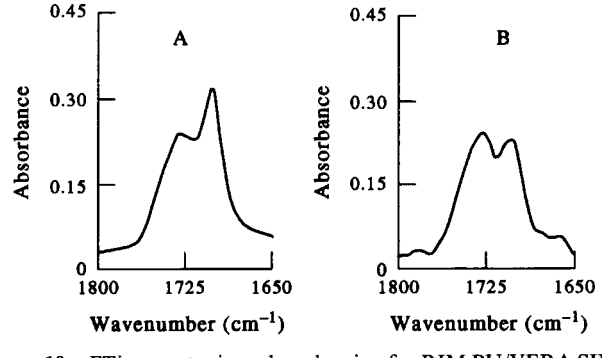

Figure 10 *FT*i.r. spectra in carbonyl region for RIM PU/VERA SINs measured at reaction time of 5 min. Left: RIM PU/VERA (53/47) SIN at 60°C; right: RIM PU/VERA (53/47) SIN at 80°C

phase separation between soft and hard segments of PU component should take place. It should be noted that although the hydrogen bonding in the carbonyl region is observed for RIM PU/VERA (53/47) SINs, the intensity of the hydrogen bonded carbonyl absorption is weaker

Table 4 Results of d.s.c. scan for RIM PU/VER SINs

Composition (PU/VER)	VERA as rigid phase			VERH as rigid phase		
	T_g (°C)	T_a (°C)	T_b (°C)	T_g (°C)	T_a (°C)	T_b (°C)
100/0	−40.5	–	175.6			
76/24	−27.0	–	170.1	−51.8[a]	–[a]	123.7[a]
61/39	−25.0	35.2	168.7			
53/47	−23.7	34.7	162.8			
40/60	−15.5	31.4	155.5	−60.6[b]	31.0[b]	112.0[b]

[a] Composition: PU/VERH (75/25), VERH-OH neglected
[b] 70% of VERH-OH counted for the extra amount of L-MDI

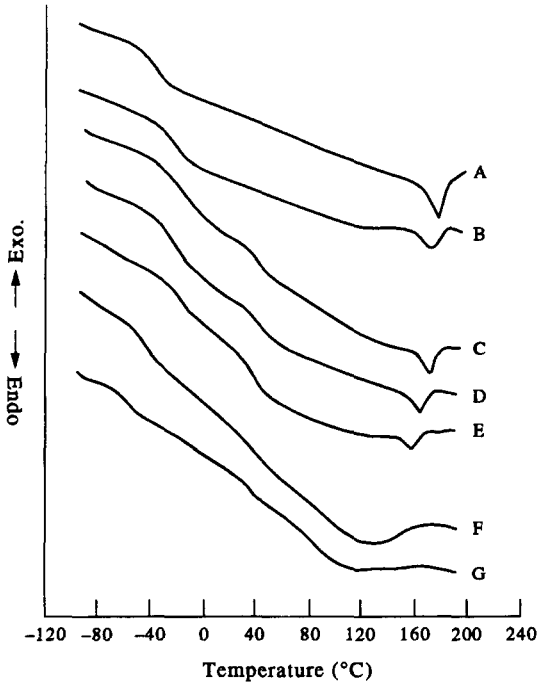

Figure 11 D.s.c. scan plots for RIM PU/VER SIN samples prepared at 60°C. PU/VERA SIN, A: 100/0; B: 76/24; C: 61/39; D: 53/47; E: 40/60; PU/VERH SIN, F: 72/25, VERH-OH neglected; G: 40/60, 70% of VERH-OH counted for the extra amount of L-MDI

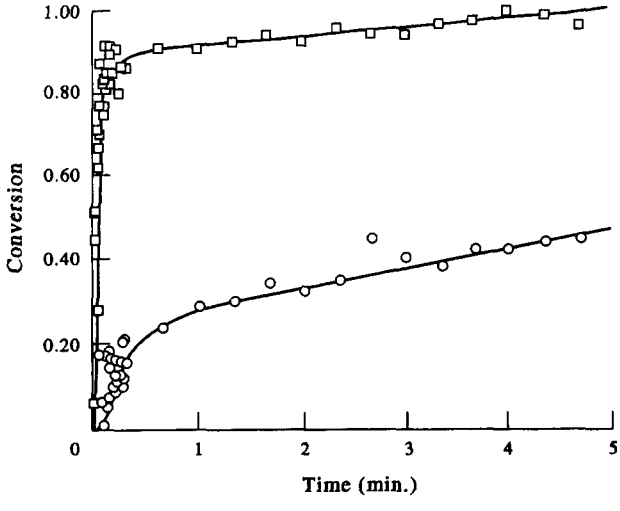

Figure 12 Isocyanate and styrene conversion in RIM PU/VERH (75/25) SIN at 80°C (VERH-OH neglected). □, NCO; ○, styrene

than that of pure PU formation at the same temperature. *Figure 11* shows the d.s.c. scan plots for RIM PU/VERA SINs with various compositions. The d.s.c. scan results are listed in *Table 4*. The low transition temperature should be ascribed to the glass transition temperature (T_g) of the soft segments in PU network[8,24,25]. The temperature of the endothermic peak (T_b) on the d.s.c. plots may be attributed to the dissociation of domains, which are composed of hard segments with long range order in the PU network[8,24–26]. There is considerable evidence in the literature[27–30] supporting the assignment of such T_bs to the melting of microcrystalline or crystalline hard segments. The other transition temperature (T_a) may be attributed to some low molecular weight styrene homopolymer or copolymer with AGC-VEO existing in the systems, as the T_a for pure PU network was not observed. With the increase of VERA proportion in RIM PU/VERA SINs, the T_g increases and the T_b decreases gradually, suggesting that the introduction of copolymerization component greatly restrains the preferential ordering process of hard segment of PU phase, leading to sharply reduced amount of crystallinity. This is consistent with the hydrogen bonding observation by using *FT*i.r. These shifts in the range of temperatures must have resulted from the interpenetration between the two networks, although the T_g for VERA network have not been detected on d.s.c. plots. All these morphological changes lead to the deviation of −NCO disappearing rate from the second order reaction kinetics at later reaction stage.

The free radical copolymerization of AGC-VEO and styrene in RIM PU/VERA (53/47) SIN system exhibits longer induction period than in pure VERA polymerization at the same temperature. Furthermore, the copolymerization would experience the strong diffusion restriction exerted by the fast formed PU network and morphological changes during the formation of RIM SINs. However, it should be noted that the styrene polymerization commences around 60% isocyanate conversion in RIM PU/VERA SIN. In this case, the vitrification of segmented PU before the isocyanate conversion required for chemical network formation is reached does play an important role in strongly restricting the diffusion of monomers in the system. Thus, all these complex changes of structure and morphology existing in the SIN system studied here render the diffusion-controlled copolymerization of AGC-VEO and styrene from the very early stage of reaction and result in the longer induction period as well as the lower conversion rate ($d\alpha/dt$) during the copolymerization, as listed in *Table 3*.

Polymerization of RIM PU/VERH SINs

RIM SINs with VERA as rigid phase can be considered to be ideal for only negligible occurrence of chemical bonds between the two networks. Then it is of interest to examine RIM SINs prepared with VERH as rigid phase, which is more close to industrial VER product.

Figures 12 and *13* display the conversion of isocyanate group and styrene comonomer for RIM PU/VERH (75/25) and (53/47) SINs, respectively. In the former case, the –OH groups on VEO backbone in VERH were neglected for the metering of L-MDI, i.e. only the –OH groups in polyether polyol and extender were counted for the amount of L-MDI; while in the later case, because of the limitation of the step variable metering ratio of the mini-RIM machine, 57% of the –OH groups on VEO backbone in VERH were considered for the extra amount of L-MDI. The urethane reaction of both systems studied exhibit much higher reactivity, compared with that of RIM PU/VERA SINs. The increase of urethane reaction rate may be attributed to the increase of the amount of hydroxyl groups existing in the systems as well as isocyanate groups. However, the nearly complete conversion of urethane reaction does not mean that the perfect structure of the soft and hard segments of PU phase could be formed, since some VEO molecules have been incorporated into the polyurethane chains[10,11].

The copolymerization of VERH reveals only a very short induction period. This experimental observation is difficult to explain presently, and should be studied further. In addition, the copolymerization of VERH in RIM PU/VERH (53/47) SIN is faster than that of VERA in RIM PU/VERA SIN of the same composition, especially at early stage (see *Figures 8* and *13*). Thus, the inter-component chemical bonds greatly influence the polymerization kinetics of RIM PU/VERH SIN systems.

Figure 14 shows that the extent of hydrogen bonding of RIM PU/VERH SIN systems is further depressed, and consequently the preferential chain ordering in PU is further suppressed. *Table 4* also lists the d.s.c. scan results of these RIM PU/VERH SINs. The even broader endothermic peaks and even lower T_bs of RIM PU/VERH SINs than those of RIM PU/VERA SINs with nearly the same composition ratio (76/24 and 40/60, respectively) indicate that the long range order composed of urethane hard segments in PU phase is not perfect enough. As a matter of fact, it has been reported that in the PU/VERH SIN systems, the isocyanate was easy to react with the –OH groups in VERH[10,11]. In other words, VEO should be easy to enter into the PU backbones. Thus, the lowering of T_bs and the higher degree of phase mixing between the two networks for the RIM PU/VERH SINs could be expected. These observations are consistent with the results of hydrogen bonding from *FT*i.r. measurements. Because of the insufficient stoichiometry of isocyanate, the rather low T_gs exhibited by the RIM PU/VERH SINs must be related to the existence of unreacted polyether polyol that has been frozen in as a result of vitrification of the systems. A T_a for PU/VERH (40/60) SIN was observed, and may also be attributed to the low molecular weight styrene homopolymer or copolymer. So far it is clear that the morphological structure of RIM PU/VERH SINs is

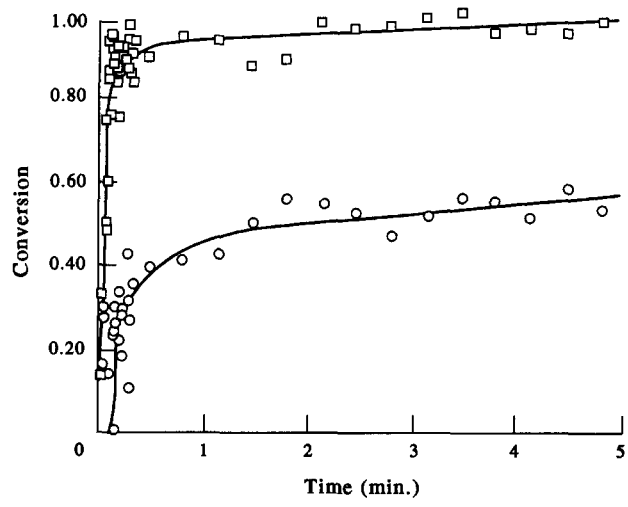

Figure 13 Isocyanate and styrene conversion in RIM PU/VERH (53/47) SIN at 80°C (57% of VERH-OH counted for the extra amount of L-MDI). □, NCO; ○, styrene

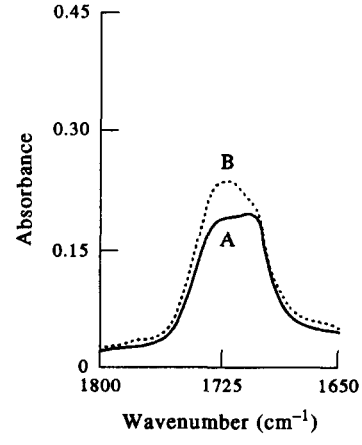

Figure 14 *FT*i.r. spectra in carbonyl region for RIM PU/VERH SINs measured at reaction time of 5 min. A, RIM PU/VERH (75/25) SIN at 80°C, VERH-OH neglected; B, RIM PU/VERH (53/47) SIN at 80°C, 57% of VERH-OH counted for the extra amount of L-MDI

hybrid and more complex than that of RIM PU/VERA SINs. The mechanical properties and morphologies of these two RIM PU/VER SINs have been examined, and found to be very different, and will be reported soon.

The knowledge of polymerization kinetics and morphology of PU/VER SIN systems synthesized in this study should be of particular value to develop and optimize the processing parameters for reinforced RIM PU materials. Much attention should be paid to the inter-component chemical binding effect if unmodified VER (with respect to the pendent hydroxyl group) is employed as the rigid phase. The very short induction period observed in RIM PU/VERH SIN systems necessitates more research effort for clear understanding. However, the formation rate of VERA network in RIM PU/VERA SIN systems studied here is not fast enough to match the RIM process and the SIN specimens should be post cured at higher temperature for longer. Thus, the other free radical initiator system should be explored further in order to speed up the copolymerization of VERA network as well as its conversion (also its crosslinking degree) before demoulding.

REFERENCES

1. Pernice, R., Frisch, K. C. and Navare, R., *J. Cellular Plast.*, 1982, March/April, 121.
2. Hsu, T. J. and Lee, L. J., *Polym. Eng. Sci.*, 1985, **25**(15), 951.
3. Yang, Y. S. and Lee, L. J., *Macromolecules*, 1987, **20**(7), 1490.
4. Kim, J. H. and Kim, S. C., *Polym. Eng. Sci.*, 1987, **27**(16), 1243.
5. Kim, J. H. and Kim, S. C., *Polym. Eng. Sci.*, 1987, **27**(16), 1252.
6. Lee, S. S. and Kim, S. C., *Polym. Eng. Sci.*, 1991, **31**(7), 1182.
7. Hsieh, K. H., Tsai, T. J. and Chang, K. W., *J. Mater. Sci.*, 1991, **26**, 5877.
8. Chen, N. P., Chen, Y. L., Wang, D. N., Hu, C. P. and Ying, S. K., *J. Appl. Polym. Sci.*, 1992, **46**, 2075.
9. Huang, X. C., Hu, C. P., Chen, Y. L., Wang, D. N. and Ying, S. K., *Polymer Material Science and Engineering* (in Chinese) 1994, **10**(3), 14.
10. Fan, L. H., Hu, C. P., Zhang, Z. P. and Ying, S. K., *J. Appl. Polym. Sci.*, 1996, **59**, 1417.
11. Fan, L. H., Hu, C. P. and Ying, S. K., *Polymer*, 1996, **37**, 975.
12. Fan, L. H., Hu, C. P. and Ying, S. K., *China Elastomerics* (in Chinese) 1995, **5**(2), 13.
13. Wu, J. G., *The Technology and Application of the Modern Fourier Transform Infrared Spectroscopy* (in Chinese). Literature Publishing House for Science and Technology, Beijing, 1994.
14. Xue, S. C., Zhang, Z. P. and Ying, S. K., *Polymer*, 1989, **30**, 1269.
15. Wang, Z. M., He, X. X. and Sun, D. Q., *The Applied Infrared Spectroscopy* (in Chinese), 2nd edn. Petroleum Industry Press, Beijing, 1990.
16. Yang, W. P. and Macosko, C. W., *Makromol. Chem., Macromol. Symp.*, 1989, **25**, 23.
17. Jin, S. R. and Meyer, G. C., *Polymer*, 1986, **27**, 592.
18. Camargo, R. E., Macosko, C. W., Tirrell, M. V. and Wellinghoff, S. T., *Polym. Eng. Sci.*, 1982, **22**, 719.
19. Bras, W., Derbyshire, G. E., Bogg, D., Cooke, J., Elwell, M. J., Komanschek, B. U., Naylor, S. and Ryan, A. J., *Science*, 1995, **267**, 996.
20. Yang, Y. S., Lee, L. J., Tomlo, S. K. and Menardi, P. J., *J. Appl. Polym. Sci.*, 1989, **37**, 2313.
21. Wang, G. C., Wang, X. and Zhang, Z. P., *Polymer Intern.*, 1991, **25**, 237.
22. North, A. M., *The Kinetics of Free Radical Polymerization*, Chapter 6. Pergamon Press, New York, 1966.
23. O'Driscol, K. F., Lyons, P. F. and Patsiga, L. R., *J. Polym. Sci.*, 1965, **A3**, 1567.
24. Zdrahala, R. J. and Critchfield, F. E., *Polym. Sci. Techn.*, 1982, **18**, 55.
25. Turner, R. B., Spell, H. L. and Vanderhider, J. A., *Polym. Sci. Techn.*, 1982, **18**, 63.
26. Seymour, R. W. and Cooper, S. L., *Macromolecules*, 1973, **6**, 48.
27. Harrell, L. L., Jr., *Macromolecules*, 1969, **2**, 607.
28. Kajiyama, T. and Macknight, W. J., *Polymer J.*, 1970, **1**, 548.
29. Chang, A. L. and Thomas, E. L., in *Multiphase Polymers*, ed. S. L. Cooper and G. M. Ester. ACS, Washington DC, 1979, pp. 31–52.
30. Hsu, T. J. and Lee, L. J., *J. Appl. Polym. Sci.*, 1987, **33**, 793.